Stereological analysis of muscle morphology following exposure to repetitive stretch-shortening cycles in a rat model

Brent A. Baker, Robert R. Mercer, Ken B. Geronilla, Michael L. Kashon, G.R. Miller, and Robert G. Cutlip

Abstract: Repetitive motion is one risk factor associated with contraction-induced muscle injury, which leads to skeletal muscle degeneration, inflammation, and dysfunction. Since current methods are unable to quantify the acute degenerative and inflammatory responses of muscle tissue concurrently, the purpose of this study was to quantify the temporal myofiber response after exposure to injurious stretch–shortening cycles (SSCs) using a standardized stereological technique. Functional testing was performed on the ankle dorsiflexor muscles of Sprague–Dawley rats in vivo. Rats were anesthetized and exposed to 15 sets of 10 SSCs. Control rats were exposed to 15 sets of single isometric contractions of the same stimulation duration. Changes in muscle morphometry were assessed at 0.5, 24, 48, 72, and 240 h post-exposure to quantify the degree of myofiber degeneration and inflammation in the tibialis anterior muscle from each group. There was an increase in the volume density and average thickness of degenerating myofibers over time in the muscle collected from rats exposed to SSCs ($p < 0.0001$) that was significantly greater than in muscle exposed to isometric contractions at 24, 48, and 72 h post-exposure ($p = 0.003$). The volume density of degenerative myofibers was associated with functional deficits at 48 h. Stereological quantification of degenerative myofibers and interstitial space changes were associated with functional defects 48–72 h after SSC-induced injury, thus demonstrating stereology is an accurate measure of SSC-induced skeletal muscle injury.

Key words: stereology, morphometry, myofiber degeneration, interstitial space, stretch–shortening cycles.

Résumé : Le mouvement répétitif est un des facteurs de risque associé aux lésions musculaires du fait même des contractions musculaires, ce qui entraîne une dégénérescence du muscle, une inflammation et une dysfonction. Les méthodes courantes ne quantifiant pas en même temps la dégénérescence et l'inflammation du tissu musculaire, cette étude se propose de quantifier l'évolution chronologique de la fibre musculaire à la suite d'une série nocive d'actions d'étirement–contraction (SSCs) du muscle, et ce, au moyen d'une technique stéréologique. L'évaluation fonctionnelle est réalisée in vivo sur les fléchisseurs dorsaux de la cheville de rats Sprague–Dawley. On soumet les rats anesthésiés à 15 séries d'actions cycliques d'étirement-contraction. Les rats témoins sont soumis à 15 séries d'actions isométriques d'une même durée. Afin de quantifier le niveau de dégénérescence et d'inflammation des fléchisseurs dorsaux de chaque groupe, les modifications myomorphométriques sont analysées 0,5, 24, 48, 72, et 240 h après les séries d'actions. On observe avec le temps une augmentation de la densité volumique et de l'épaisseur moyenne des fibres en dégénérescence dans les muscles des rats soumis aux actions cycliques d'étirement-contraction ($p < 0{,}0001$); cette augmentation est significativement plus importante que celle observée dans les muscles soumis aux actions isométriques 24, 48, et 72 h après coup ($p = 0{,}003$). La densité volumique des fibres en dégénérescence est associée aux déficits fonctionnels observés 48 h après les séries d'actions. La quantification stéréologique des fibres musculaires en dégénérescence et les modifications du milieu interstitiel sont associées aux déficits fonctionnels observés 48 à 72 h après les séries d'actions nocives de SSC; la stéréologie permet donc de mesurer avec précision les lésions dues aux SSC.

Mots clés : stéréologie, morphométrie, dégénérescence myofibrillaire, milieu interstitiel, actions cycliques d'étirement-contraction.

[Traduit par la Rédaction]

Received 21 January 2005. Accepted 27 April 2005. Published on the NRC Research Press Web site at http://apnm.nrc.ca on 1 March 2006.

B.A. Baker, R.R. Mercer, K.B. Geronilla, M.L. Kashon, G.R. Miller, and R.G. Cutlip.[1] National Institute for Occupational Safety and Health (NIOSH), Health Effects Laboratory Division, 1095 Don Nehlen Drive, M/S 2027, Morgantown, WV 26505, USA.

[1]Corresponding author (e-mail: rgc8@cdc.gov).

Introduction

A variety of methods have been used to examine the physiological and cellular responses to contraction-induced muscle injury. Exposure to concentric (shortening) or isometric muscle actions does not normally produce muscle injury (Warren et al. 1993*a*, 1999; Faulkner et al. 1995; Lieber et al. 1996). However, exposure to eccentric contractions has been shown to result in an isometric force deficit (Warren et al. 1999), structural disruption at the cellular level, and

 doi:10.1139/H05-009

cellular infiltrates as a result of an inflammatory response (Warren et al. 1999; Lieber et al. 1996; Faulkner et al. 1989; Warren et al. 1993*b*; Friden et al. 1983; McCully and Faulkner 1985). Even though numerous models have been used to study the functional and biological mechanisms of contraction-induced muscle injury, there is a paucity of studies quantifying both skeletal muscle damage and inflammation after contraction-induced muscle injury (Koh et al. 2003; Geronilla et al. 2003). The ability to rapidly quantify both skeletal muscle degeneration and inflammation in the same tissue following an injurious exposure would yield further insight into the injury and repair process of skeletal muscle. It has been shown that exposure to injurious eccentric muscle actions results in disruption of the cellular membrane, loss of intermediate filaments and structural proteins, and the influx of extracellular proteins into the cell (Komulainen et al. 1998, 2000; Friden and Lieber 1998; Lieber et al. 1994). Sarcomeric lesions, disorganized actin, and Z-disc streaming also result after injury (Stupka et al. 2001; Vijayan et al. 2001; Devor and Faulkner 1999; Lieber et al. 1991). During the injury process, damaged cells lose apposition to neighboring cells and there is evidence of cellular infiltrates such as neutrophils and macrophages entering the damaged cells (Koh et al. 2003; Devor and Faulkner 1999). Days after injury, the regenerative process is initiated and central nuclei appear present (Bigard et al. 1997; Hesselink et al. 1996). At this time, the muscle demonstrates a mixture of both degenerative and regenerative processes.

Three distinct methods have been used to quantify muscle damage: (*i*) using the percent of injured fibers (Koh et al. 2003; Faulkner et al. 1989; Van Der Meulen et al. 1997), the area fraction of damaged fibers (McCully and Faulkner 1986; Lieber and Friden 1993), or the number of damaged fibers (Devor and Faulkner 1999); (*ii*) using the number or percentage of fibers affected by a change in the structural proteins (desmin, fibronectin, and dystrophin), which is indicative of damage, or using the number of fibers that have central nuclei, which is indicative of regeneration (Hesselink et al. 1996; Koh et al. 2003; Komulainen et al. 2000); and (*iii*) muscle ultrastructure disruption as classified by fibers with sarcomeric lesions (Komulainen et al. 1998; Lieber and Friden 1993; Lieber et al. 1996).

However, these methods have not established strict classification criteria for quantifying myofiber damage. Contraction-induced models have been used to study muscle damage in extensor digitorum longus (EDL) and tibialis anterior (TA) muscles in rats (Van Der Meulen et al. 1997), mice (Koh et al. 2003), and rabbits (Lieber and Friden 1993). Classification criteria for damaged vs. non-damaged fibers in these studies included myofiber swelling, degenerative changes such as pale or discontinuous staining of the cytoplasm, the presence of infiltrating inflammatory cells, and the state of cell nuclei (Devor and Faulkner 1999; Koh et al. 2003; Van Der Meulen et al. 1997; McCully and Faulkner 1986; Lieber and Friden 1993; Faulkner et al. 1989). Whereas these approaches were well suited for the overall assessment of muscle damage, they did not lend themselves to quantitative assessment of the myofiber injury present. Additionally, these methods did not address the interstitial space's responses and modifications to the induced injury.

Even though there are benefits to investigating muscle damage with the existing morphological procedures, there are clear and distinct limitations to the current approaches. Even though it is well recognized that myofiber degeneration occurs and that interstitial space components participate in both degeneration and the inflammatory process, neither degeneration nor inflammatory components are fully understood. For this reason it was imperative to use a standardized technique that enabled rapid and concurrent quantification of degeneration and inflammation (Krajnak et al. 2004). Thus, the purpose of the present study was to systematically quantify skeletal muscle degeneration and changes occurring to the interstitial space, which could be related to the changes in muscle performance. To accomplish this, we determined the morphological properties of normal and degenerative myofibers based on a rigorous set of definitions and quantified the corresponding changes in the myofiber and the interstium using a standardized stereological method (Underwood 1970). We hypothesized that indices of myofiber degeneration and inflammation, as well as modifications observed in the interstitial space, would increase temporally as a result of the stretch–shortening (SSC)-induced muscle injury. To determine if these quantitative measures of muscle morphology paralleled corresponding changes in muscle physiology, measurements of muscle functional properties were made. For this purpose animals were tested using a custom-built dynamometer (Cutlip et al. 1997), which regulated muscle contraction and recorded muscle output parameters produced by electrical stimulation of rat dorsi flexor muscles in vivo.

Materials and methods

Animals

Male Sprague–Dawley rats (n = 72; 422 ± 19 g, 12 weeks of age) were housed in an Association for Assessment and Accreditation of Laboratory Animal Care approved animal quarters where the temperature and a 12 h light : 12 h dark (0700 to 1900 h) cycle were held constant and food and water were provided ad libitum. All rats were exposed to a standardized experimental protocol that complied with the Guidelines for the Care and Use of Laboratory Animals, which was approved by the National Institute for Occupational Safety and Health Animal Care and Use Committee. Animals were randomly assigned to either an isometric control group (CON group, n = 36) or a stretch–shortening cycle group (SSC group, n = 36). Each group was then randomly subdivided into 0.5, 6, 24, 48, 72, or 240 h recovery groups (n = 6). A subset of animals, which constituted the CON group at 0.5 and 48 h and the SSC group at 0.5- and 48-h recovery, were reported in a previous study (Geronilla et al. 2003).

Experimental setup

Animals were tested on a custom-built rodent dynamometer as previously described (Cutlip et al. 1997). Rat TA muscles were exposed to an SSC protocol as previously described by Geronilla et al. (2003). Briefly, rats were anaesthetized with isoflurane gas in an induction tank (Surgivet Anesco Inc., Waukesha, Wis.) and placed supine on the

Table 1. Absolute and relative left tibialis anterior (LTA) muscle masses.

(*a*) CON group (recovery (h))	LTA absolute muscle mass (mg)	LTA relative muscle mass (mg/100 g body mass)
0.5	831±37.0	196±7.8
6	864±19.3	202±3.1
24	864±22.2	202±6.6
48	797±15.8	193±5.3
72	792±14.0	187±0.9
240	899±33.7	202±5.8
(*b*) SSC (recovery (h))	LTA absolute muscle mass (mg)	LTA relative muscle mass (mg/100 g body mass)
0.5	819±23.9	197.2±5.8
6	907.3±47.9	212±4.9
24	938±21.1	220±2.3
48	963±23.5	229±8.5
72	870±20.8	205±7.1
240	801±41.7	184±7.0

Note: The LTA absolute and relative muscle masses are shown as mean ±SE. Each row signifies the respective muscle wet masses at the specified sacrifice time point. The upper panel of the table represents the isometric-control (CON), whereas the lower panel of the table represents the stretch–shortening cycle (SSC) group.

heated *x*–*y* positioning table of the rodent dynamometer with an anaesthetic mask over the nose and mouth. The knee was secured with a knee holder and the left foot was secured in the load cell fixture with the ankle axis (assumed to be between the medial and lateral malleoli aligned with the axis of rotation of the load cell fixture). Each animal was monitored during the procedure to maintain proper anaesthetic depth and body temperature.

Functional testing

Platinum stimulating electrodes (catalogue No. F-E2, Grass Medical Instruments, Quincy, Mass.) were placed subcutaneously to span the common peroneal nerve. Activation of the electrical stimulator resulted in muscle contraction of the dorsi flexor muscle group. Stimulator settings were optimized to maximize dorsi flexor contractile performance as previously described (Geronilla et al. 2003; Cutlip et al. 2004). Muscle stimulation for all protocols was conducted at 120 Hz stimulation frequency, 0.2 ms pulse duration, and 4 V in magnitude. The joint angle of the rat ankle was defined as the angle between the tibia and the plantar surface of the foot. The angular position of the load cell corresponded with the foot position. Vertical forces applied to an aluminum sleeve fitted over the dorsum of the foot were translated to a load cell transducer (Sensotec, Inc., Columbus, Ohio) in the load cell fixture. The force produced by the dorsiflexor muscles was measured at the interface of the aluminum sleeve and the dorsum of the foot. An isometric contraction was performed with the ankle at an angle of 1.57 rad (1 rad = 57.3°) using 300 ms stimulation duration. An isometric contraction was performed 2 min before (pre) and 2 min after (post) either 15 sets of 10 stretch–shortening contractions (SSC group) or 15 isometric contractions (CON group) and before sacrifice at 0.5, 6, 24, 48, 72, or 240 h. All animals were returned to their home cages in the animal quarters after their respective treatment protocol and remained there with access to food and water ad libitum until time of sacrifice. Animals were monitored by the National Institute for Occupational Safety and Health animal quarters staff after their treatment exposure and did not show any signs of distress.

Injury protocol

The SSC group was exposed to 15 sets of SSCs. The SSCs were performed by full activation of the dorsi flexor muscles for 100 ms and then moving the load cell fixture from 1.13 rad to 2.00 rad angular position at a velocity of 8.72 rad/s, in a reciprocal fashion, for 10 oscillations. After 10 oscillations, the load cell fixture was stopped at angular position 1.13 rad and the dorsi flexor group was deactivated 300 ms later. The total stimulation time per set was 2.8 s. The 15 sets of 10 oscillations were conducted at 1 min intervals.

Isometric control protocol

The CON group was exposed to 15 isometric contractions at 1 min intervals. During each contraction, dorsi flexor muscles were stimulated for 2.8 s at 1.57 rad using the same stimulation parameters and duration as in the SSC group.

Histology

Following completion of the 2nd post-test rats from both the CON group and SSC group were weighed, anesthetized with sodium pentobarbital (i.p., 10 mg/100 g body mass) and exsanguinated at 0.5, 6, 24, 48, 72, and 240 h after exposure. The left tibialis anterior (LTA) muscle was dissected, cleaned, and weighed (see Table 1 for absolute and relative muscle wet masses). The midbelly region was cut from the muscle and mounted on cork, immersed in optimal cutting temperature (OCT) medium, frozen in isopentane cooled with liquid nitrogen, and stored at –80 °C. The midbelly region was selected to obtain the maximum tissue sample. Transverse sections were cut at 12 microns (μm), mounted on precoated microscope slides, air dried, and stained with Harris hematoxylin and eosin using a routine procedure. Permount was used to attach coverslips to the microscope slides. Stereological analyses were evaluated on a Leica DMLB microscope (Wetzlar, Germany).

Myofiber definitions

Stereology was used to quantify the degree of myofiber degeneration and the accompanying changes in the interstitial space in the TA muscle from each group. Myofibers were defined by the following criteria: normal myofibers demonstrated (*i*) complete contact with adjacent myofibers, (*ii*) a smooth outer membrane, and (*iii*) no presence of internal inflammatory cells; degenerative myofibers displayed (*i*) a loss of contact with adjacent myofibers, (*ii*) presence of internal inflammatory cells, and (*iii*) an outer membrane interdigitated with inflammatory cells (Fig. 1).

Stereology

Quantitative morphometric methods were used to measure the volume fraction, surface densities, and average thickness of normal myofibers, degenerative myofibers, and the

Fig. 1. Examples of myofiber definitions. The top 3 light micrographs illustrate the typical close apposition and smooth membrane profiles of normal myofibers (arrows). The 3 lower profiles illustrate the loss of contact with neighboring myofibers (arrows), which was one criterion used to define degenerative myofiber profiles. As illustrated, these myofibers also displayed a highly ruffled outer membrane, which was interdigitated with inflammatory cells.

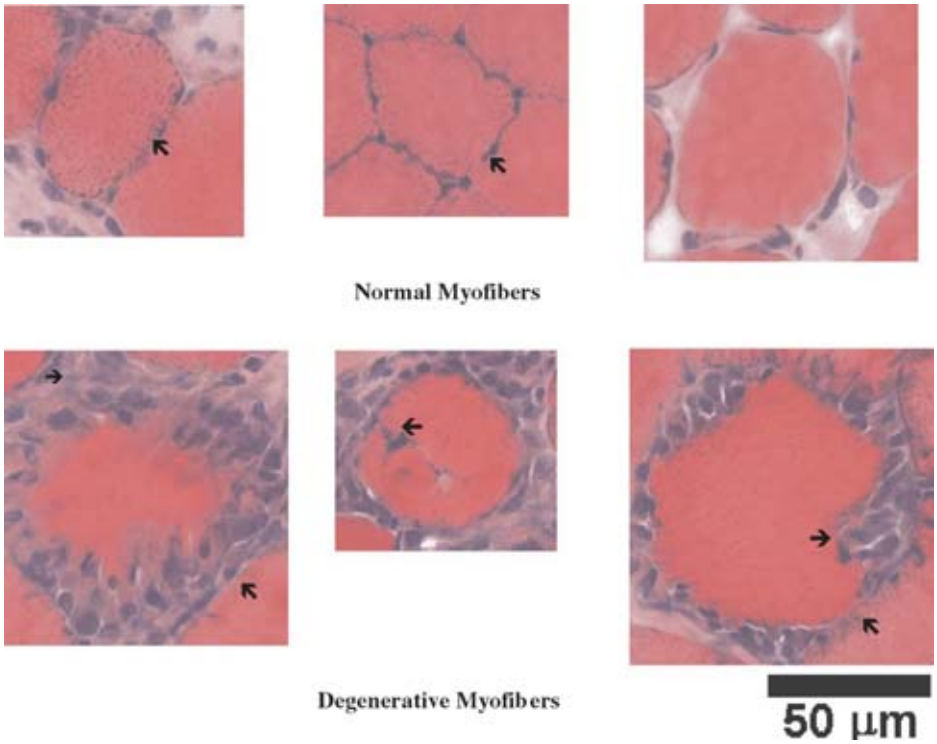

Fig. 2. Isometric force changes in the isometric control groups (CON) and stretch–shortening groups (SSC) after injury. The effect of exposure to SSCs on change in isometric forces generated by the dorsi flexors from 0.5 to 240 h after exposure was significantly different from those forces resulting from exposure to isometric contractions. Asterisk indicates significant differences at $p < 0.0016$. Data shown are mean ± SE.

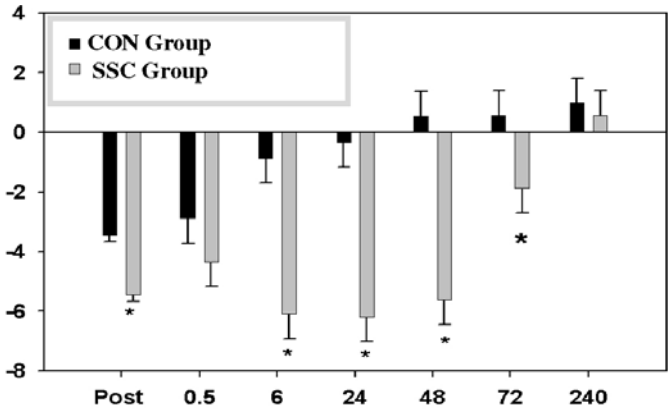

interstitial space as previously described (Underwood 1970). The interstitium was divided into the endomysium and the perimysium space, which included the capillaries. Stereology was also used to quantify the degree of inflammation, which was quantified as either non-cellular interstitium (NCI) indicative of edema, or cellular interstitium (CI); CI consisted of all possible infiltrating cells including, but not limited to, inflammatory cells, endothelial cells, and fibroblasts. Again, volume and surface density were measured using standard morphometric analyses (Underwood 1970). A stage micrometer was used to identify the mid-point of the sample section. Point and intercept counts using a 121-point, 11-line overlay graticule (12.5 mm square with 100 divisions) at 40× magnification were taken at 5 equally spaced sites across the section. This process was repeated 2 mm on either side of the midpoint of the section for a total of 1210 points and 110 intercept lines per section. Volume density or the percent tissue volume (%volume) were computed from the percentage of points over the tissue section to points over normal myofibers, degenerative myofibers, CI, and NCI plus capillaries. Intercepts over the line overlay were counted for the perimeter of normal myofibers, degenerative myofibers, and interstitium to myofiber transitions. Points and intercepts over blood vessels greater than 25 µm in diameter were excluded. Average thickness or average distance were computed as twice the ratio of volume to surface density according to standard morphometric analysis (Underwood 1970).

Statistical analysis

Statistical analyses were conducted using SAS version 8 (SAS Institute Inc., Cary, N.C.). Muscle masses of the left tibialis anterior and isometric force data (difference in isometric force generated between the pre-test and the tests during the recovery period) were analyzed with 2-way analyses of variance (ANOVAs). Where appropriate, post-hoc comparisons were conducted using Fisher's least significant

Fig. 3. Wet mass of the left tibialis anterior (LTA) muscle (standardized to 100 g body mass) in animals exposed to isometric control (CON) or stretch-shortening cycle (SSC) protocols. There was a significant interaction between experimental treatment and recovery time on left tibialis anterior muscle weights ($p = 0.0007$). At 24, 48, and 72 h, the SSC groups had significantly higher muscle mass than did the CON groups. At 240 h, this difference was reversed. Data shown are mean ± SE. Asterisk indicates significantly different from CON groups relative to the same time points at $p < 0.05$.

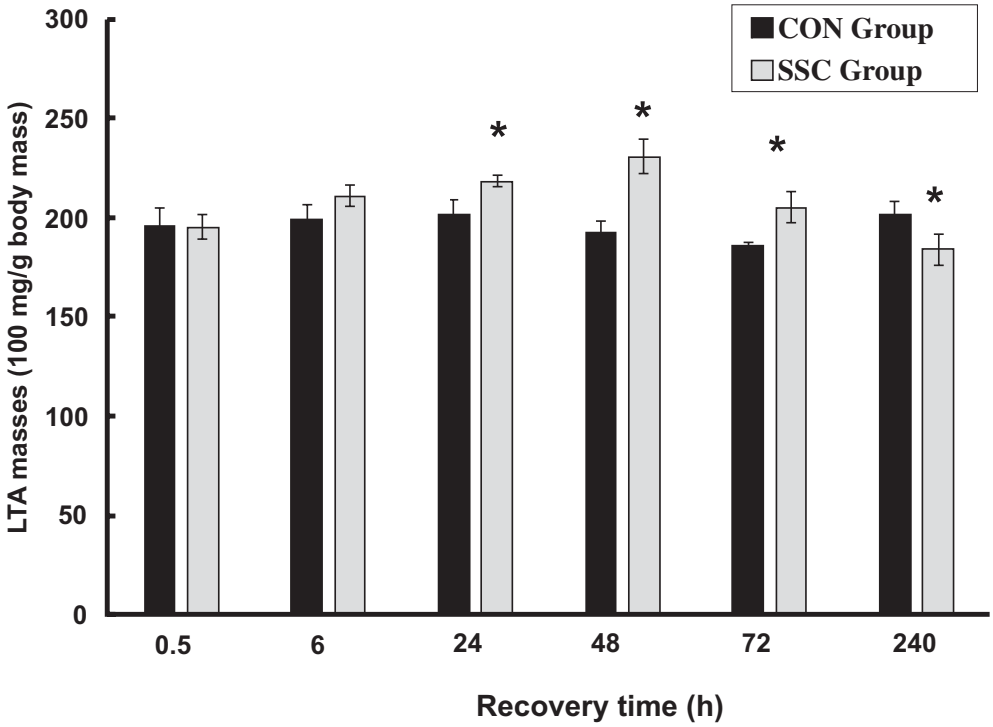

difference tests. Stereological measurements of the volume and thickness of cellular and noncellular components were analyzed using 2-way (treatment × time) ANOVAs. Post-hoc comparisons were made using Fisher's least significant difference tests. Since the data was deemed ordinal, a non-parametric correlation coefficient was implemented to assess the relationships between force, volume, and thickness. Therefore, to compare measurements of percent force drop, %volume degenerative myofiber, %volume NCI, and %volume CI in CON-group and SSC-group animals, Spearman's ρ was used for analyses of data, and results were reported via the Spearman's coefficient of rank correlation (r_s). One section per animal with 6 animals per group was evaluated and the results expressed as mean ± SE.

Results

Analyses of isometric force deficits

The isometric force decrement between the pre- and post-tests in both the SSC and CON groups are shown in Fig. 2. There was a significant interaction between experimental treatment and recovery time ($p = 0.0016$). Comparisons at each time point show that the isometric force decrement is significantly greater for the SSC group than the CON group at 6, 24, 48, and 72 h (Fig. 2). In both groups, there was an initial force decrement, which persisted for at least 30 min. However, in the CON group, the force decrement rapidly approaches baseline values by 6 h (the 0 time point is within the 95% confidence interval around the point estimate); in the SSC group, this does not occur until 240 h. Total recovery from contraction-induced injury was observed at 240 h, which was recognized by no difference in isometric post-test and pre-test forces (Fig. 2).

Analyses of TA muscle wet masses

Weights of the LTA muscles (normalized to body mass) are shown in Fig. 3. There was a significant interaction between experimental treatment and recovery time ($p = 0.0007$). Analyses revealed that at 24, 48 and 72 h, the SSC groups had significantly higher muscle masses than the CON groups ($p < 0.05$). However, at 240 h this difference was reversed ($p = 0.024$), with the muscle masses in the CON group being higher than masses in the SSC group. There were no statistically significant differences in the body mass of treatment groups prior to the application of treatments ($p = 0.6148$), and thus these differences in LTA masses cannot be attributed simply to differences in body mass.

Analyses of temporal TA muscle response

Tissue sections from the 72 h CON group showed normal myofiber morphometry (Fig. 4*a*). In addition, the 240 h CON group also showed normal fiber morphometry (Fig. 4*b*). All tissue sections from the 72 h SSC group showed evidence of extensive interstitial swelling of the perimysium and endomysium (NCI), and interstitial hypercellularity (CI), as well as degenerative myofibers (Fig. 4*c*). The 240 h SSC group had numerous myofibers with central nuclei, which was indicative of a degenerative–regenerative process (Fig. 4*d*).

Fig. 4. Morphological changes in muscle tissue after exposure to isometric or stretch–shortening protocols (SSCs). (*a*) Tissue sections from the 72-h isometric control group showed normal myofiber arrangement. (*b*) The 240-h isometric control group also showed normal fiber arrangement. (*c*) All tissue sections from the 72 h SSC-exposed group showed extensive interstitial swelling of the perimysium and endomysium NCI (non-cellular interstitium), swollen myofibers, interstitial hypercellularity owing to CI (cellular interstitium), and degenerative myofibers (asterisk). (*d*) The 240 h SSC-exposed group had numerous fibers with central nuclei (CN) and virtually no remaining degenerative fibers. The scale shown is 100 µm.

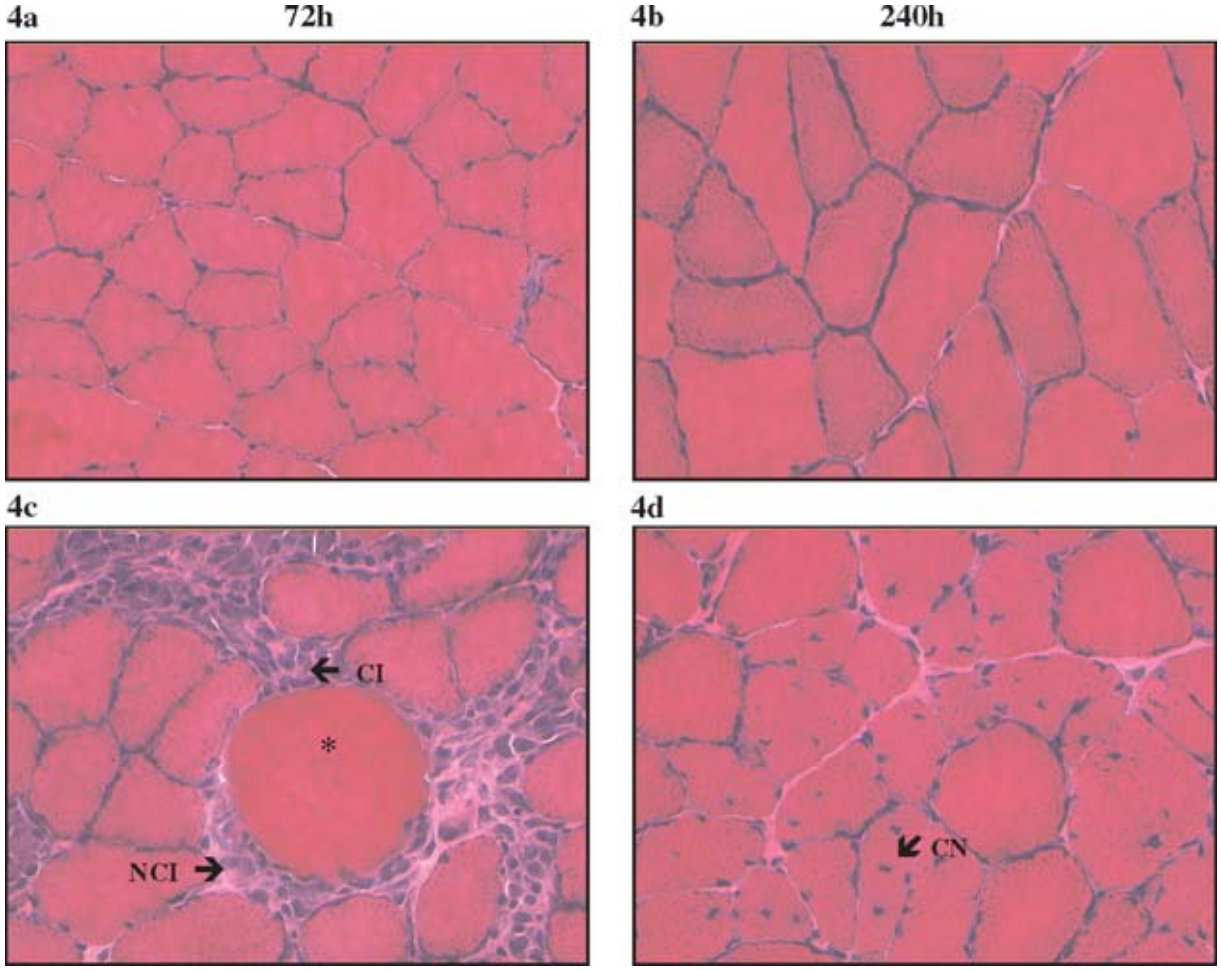

Stereological analyses of myofiber degeneration

Statistical analyses for measurements of degeneration showed that there were no degenerative myofibers present in muscle collected from animals in either of the CON groups. In contrast, there was an increase in the %volume and average thickness of degenerating myofibers over time in the muscle collected from rats exposed to the SSC protocol ($p < 0.0001$). Further analyses revealed that the %volume and average thickness of degenerating myofibers from muscle exposed to the SSC protocol was significantly greater than muscle exposed to isometric contractions at 24, 48, and 72 h post-exposure (Figs. 5 and 6), respectively ($p = 0.003$). There were no degenerative myofibers seen in muscle 240 h post-exposure.

Stereological analyses of inflammation

Stereological estimates of inflammation and changes that occurred in the interstitial space were also analyzed. The 2-way ANOVA analyzing the %volume of the NCI produced a treatment × time interaction ($p = 0.009$). Further analyses revealed that the %volume of the NCI was higher in the SSC group 48 h post-exposure than in the CON group (Fig. 5; $p < 0.0001$). This is consistent with the increased edema seen in injured tissue collected at this time point (Geronilla et al. 2003). Measuring the %volume of the CI and the average thickness of the interstitial space quantified cellular inflammation. The 2-way ANOVAs for these variables produced treatment × time interactions (volume, $p < 0.0001$; thickness, $p < 0.0001$). Post-hoc comparisons revealed that the %volume of CI was higher in muscles exposed to the SSC protocol 48 h ($p < 0.0001$) and 72 h ($p < 0.0001$) post-exposure than in the muscles of animals in the CON groups (Fig. 5). The average thickness of the interstitial space also was higher in muscle exposed to the SSC protocol than in muscle from the CON group rats 48 ($p < 0.0001$) and 72 h ($p < 0.0001$) post- injury (Fig. 6). These data are consistent with the presence of swollen and necrotic myofibers in injured tissues at these time points (Geronilla et al. 2003).

Fig. 5. The volume of cellular and non-cellular components of muscle exposed to isometric (CON) or stretch-shortening cycle (SSC) contractions. Isometric contractions did not significantly alter the interstitial space or produce the formation of degenerative myofibers. In contrast, exposure to SSCs resulted in increased volume of tissue occupied by degenerative myofibers (Deg. Myo), cellular interstitium (CI), and non-cellular interstitium (NCI). Asterisk indicates significantly greater than isometric control group muscles relative to the same time point at $p < 0.01$.

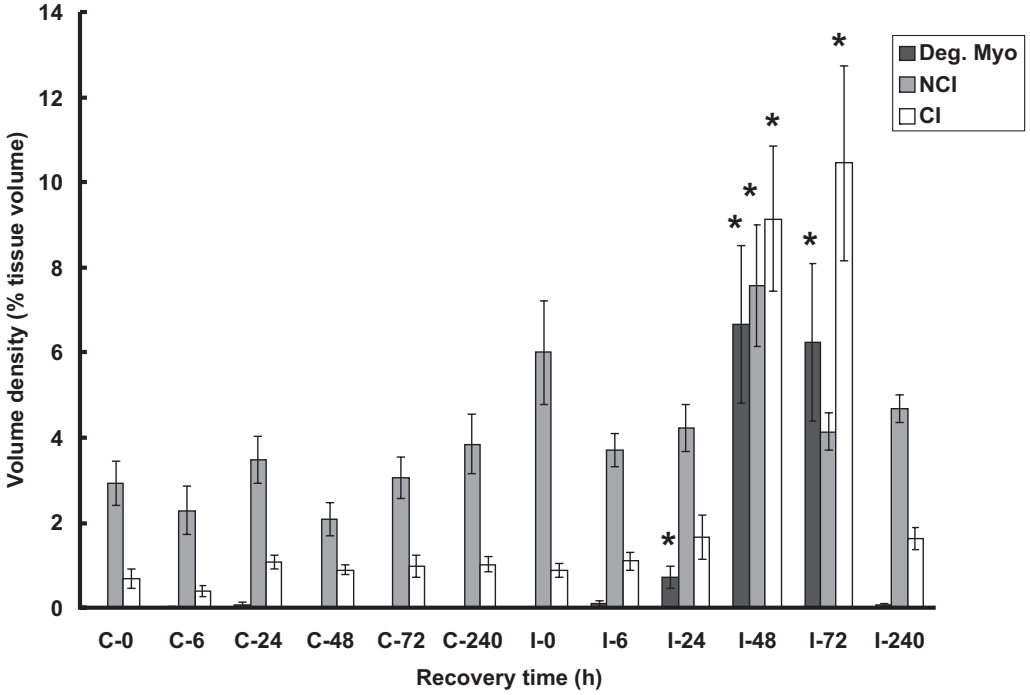

Response kinetics for function vs. %volume or average thickness

In TA muscles for which contractile and stereological analyses were performed after exposure to SSC contractions, response kinetics were profiled for degeneration and inflammation, respectively (Figs. 7*a*, 7*b*, and 8*a*–8*c*). Figure 7*a* depicts the response kinetics for the percent force drop versus the percent degenerative myofiber volume. Since the percent force drop curve was identical in all profiles, this kinetic profile was repeated in all figures. The percent force drop was affected most significantly from 0.5 to 48 h, but returned towards baseline by 240 h; the percent degenerative myofiber volume displayed a significant increase at 24 h and 72 h after SSC exposure. The percent degenerative myofiber volume returned towards baseline by 240 h. In Fig. 7*b*, the response kinetics for percent force drop vs. the average degenerative thickness was illustrated. Once again, we see a very modest increase at early time points (0–6 h), but a significant increase in the average degenerative thickness between 24 and 72 h. However, at 240 h, we do not see a return to baseline in the average degenerative thickness.

Figures 8*a* and 8*b* illustrate the response kinetics for the percent force drop compared with the percent NCI and percent CI volume, respectively (%volume NCI and %volume CI). The %volume NCI displayed a significant increase at 48 h. The %volume NCI remained elevated at 72 and 240 h. Figure 8*b* illustrates that at the early time points, 0.5–24 h, no significant changes in percent CI were observed. At 48 h and 72 h, a significant increase in the %volume CI was observed, which, as seen in the NCI, remained elevated at 240 h. In Fig. 8*c*, no change in the thickness of the interstitial space was detected between 0.5 and 24 h, but a significant increase in the thickness of the interstitial space was observed at 48 h and 72 h. By 240 h post-injury, the thickness of the interstitial space had returned to sub-baseline values.

Correlations of isometric force drop percent, volume density, and average thickness

In TA muscles for which contractile and stereological analyses were performed after exposure to either SSC contractions or isometric contractions, correlations were present. A negative correlation was observed between percent force drop and percent degenerative myofiber volume in the SSC group 48 h post-injury, $r_s = -0.77$ (illustrated in Fig. 7*a*). Also, a negative correlation was observed between the percent force drop and the %volume NCI of the SSC group 72 h post- injury, $r_s = -0.66$ (illustrated in Fig. 8*a*). In addition, percent force drop and %volume CI showed a positive correlation 48 h post-injury, $r_s = 0.77$ (illustrated in Fig. 8*b*).

Discussion

The major findings of this study were that levels of myofiber degeneration, inflammation, and related changes in the interstitial space were quantifiable using this standardized stereological technique (Krajnak et al. 2004). Additionally, we show degenerative myofibers and interstitial changes were associated with functional performance temporally. Specifically, our working hypothesis was supported and our results were indicative of increased temporal indices of degeneration and inflammation; these measures were associated with functional performance. These results are in

Fig. 6. The thickness of degenerative myofibers and the interstitial space of muscle exposed to isometric (CON) or stretch–shortening cycle (SSC) contractions. The thickness of degenerative myofibers (Deg. Myo) and the interstitial space response after exposure to SSC. Asterisk indicates significantly greater than isometric control group relative to the same time point at $p < 0.01$. These variables are not affected by exposure to isometric contractions.

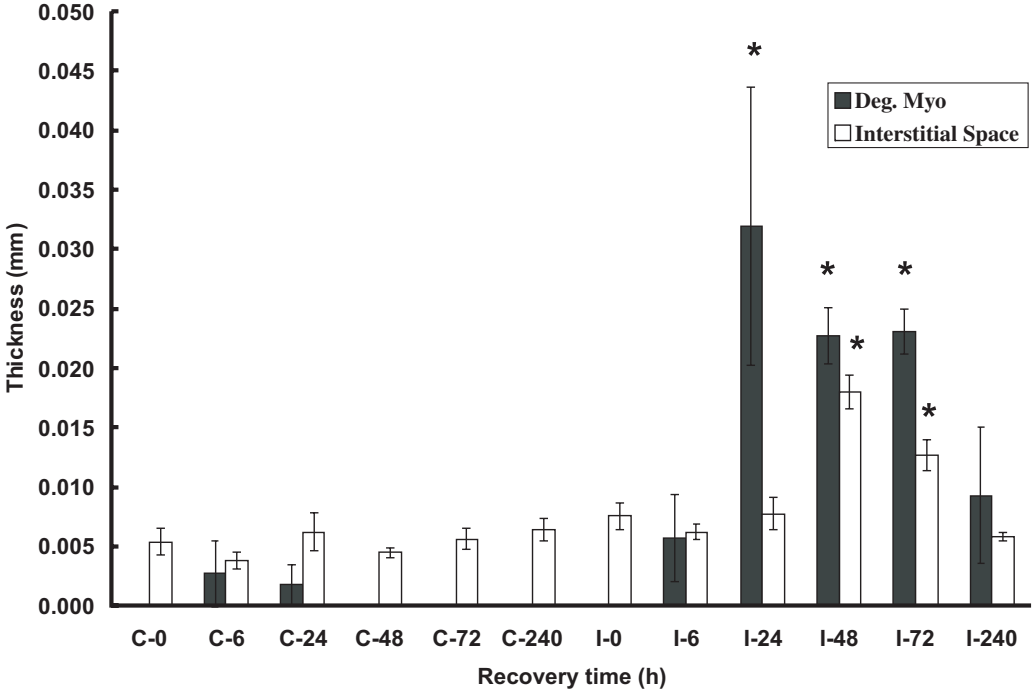

agreement with data shown in previous investigations (McCully and Faulkner 1985, 1986), yet the majority of previous studies (Devor and Faulkner 1999; Van Der Meulen et al. 1997; Lieber and Friden 1993) are limited by having reported the number, percent, or cross-sectional area of damaged fibers at single time points following exposure. Also, previous histological studies have failed to directly quantify myofiber degeneration and its relationship to evident functional deficits following contraction-induced exposure. While the ability to characterize early-phase muscle damage is a fundamental benefit of immunohistochemical techniques, a lack of agreement in the extent of muscle damage reported morphologically and the magnitude of force loss still exists (Komulainen et al. 1998, 2000; Friden and Lieber 1998).

An important aspect in quantifying skeletal muscle's degenerative response is that the reported biological changes, although small, may be extremely significant functionally. Since we are comparing significant increases and (or) decreases to a control group that is not being affected, changes in vivo should not be discounted because they do not compare well with in vitro or in situ values that have been reported. In contrast, the capacity to detect significant changes and associations with functional measures illustrates how highly sensitive this piece of biological evidence is and should not be disregarded. By establishing rigorous exclusion criteria for categorizing cellular normality, degeneration, and inflammation, we were able to objectively determine the histological status of the muscle temporally after an injurious SSC exposure.

It was essential to devise a rapid method in which the most naïve examiner would be proficient in establishing highly reproducible results and would be able to verify the results, since observer and sampling biases do yield varied results (Glaser 2000). Further comparisons, which were based on a review of the literature by Warren and colleagues (Warren et al. 1999) in which histological methods were used in previous studies, have shown the inability to overcome researcher and (or) observer bias or sampling error, thus relating the extent of muscle damage morphologically to functional deficit. This may be predominantly due to sampling methods and classification techniques. Without implementing stringent classification criteria used to quantify the myofiber's response to a given exposure, inadequacies often exist. Various instances arise where fibers appear to be histologically damaged; however, there may be no noted functional impairment because the force deficit observed was due to fatigue only (Vijayan et al. 2001). As a result, disconnects appear when attempting to relate muscle damage incurred at the ultrastructural level to function and, in the majority of the cases, the interstitium's involvement is not detailed (Stupka et al. 2001). Early, single, time points used for histological and (or) morphological samples have been shown to be problematic and do not relate to the time course observed for decrements in contractile properties. Consequently, the capacity to characterize ultrastructural events and objectively quantify and (or) predict myofiber degeneration and functional decrements may be limited. In the current study, the stereological measurements of myofiber degeneration and the concomitant changes observed with the

Fig. 7. (*a*) Response kinetics for the percent force drop vs. percent tissue volume of degenerative (Vol. Deg.) myofibers for stretch–shortening cycle (SSC)-exposed groups. Circled variables and asterisk illustrate observed correlation between percent force drop and percent tissue volume of degenerative myofibers. (*b*) Response kinetics for the percent force drop versus the average thickness of degenerative myofibers for SSC-exposed groups.

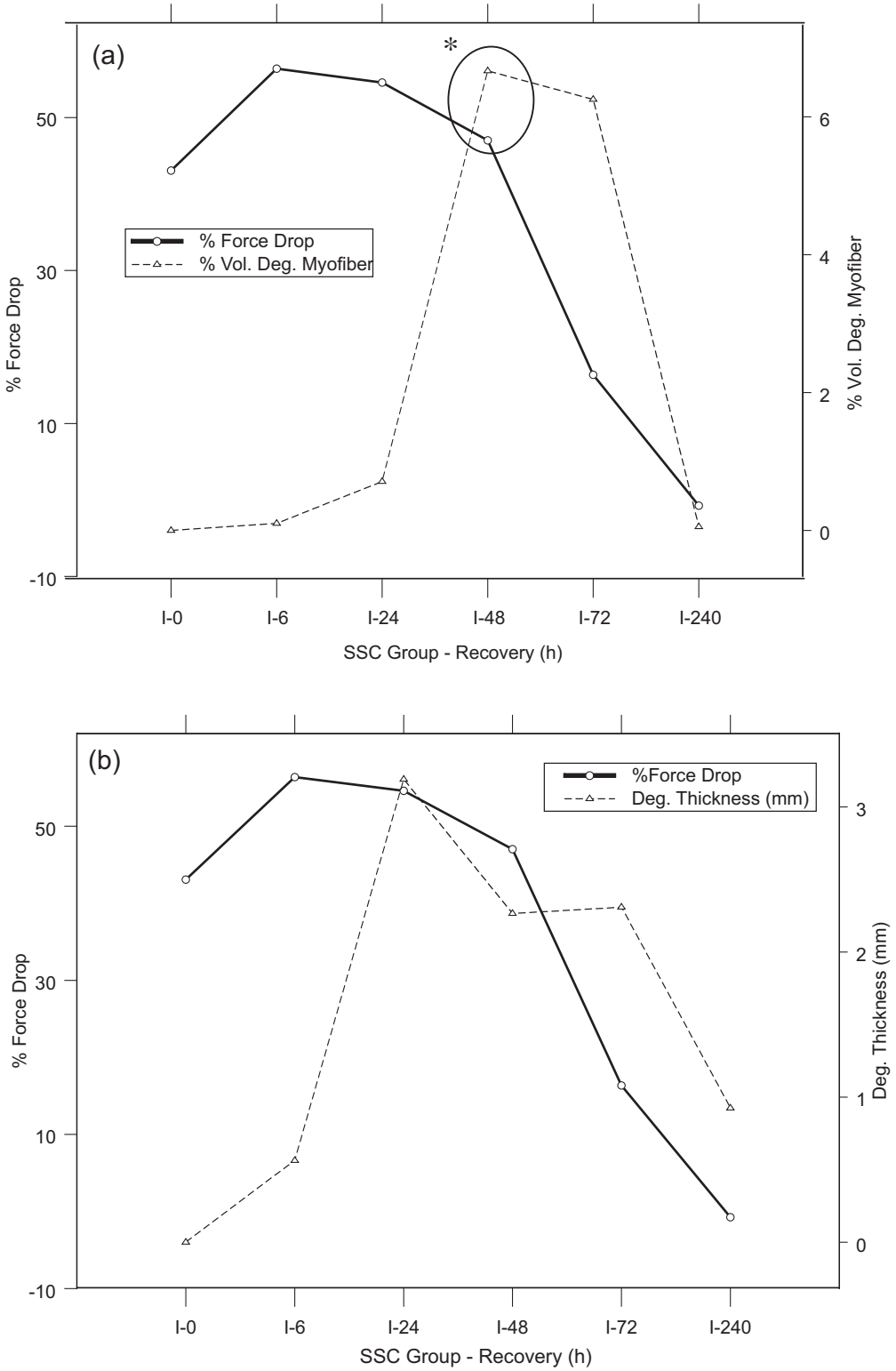

Fig. 8. (*a*) Response kinetics for the percent force drop versus percent tissue volume of non-cellular interstitium (NCI) for stretch–shortening cycle (SSC)-exposed groups. Circled variables and asterisk illustrate observed correlation between percent force drop and percent tissue volume of NCI. (*b*) Response kinetics for the percent force drop versus percent tissue volume of cellular interstitium (CI) for SSC-exposed groups. Circled variables and asterisk illustrate observed correlation between percent force drop and percent tissue volume of CI. (*c*) Response kinetics for the percent force drop vs. average thickness of the interstitial space for SSC-exposed groups.

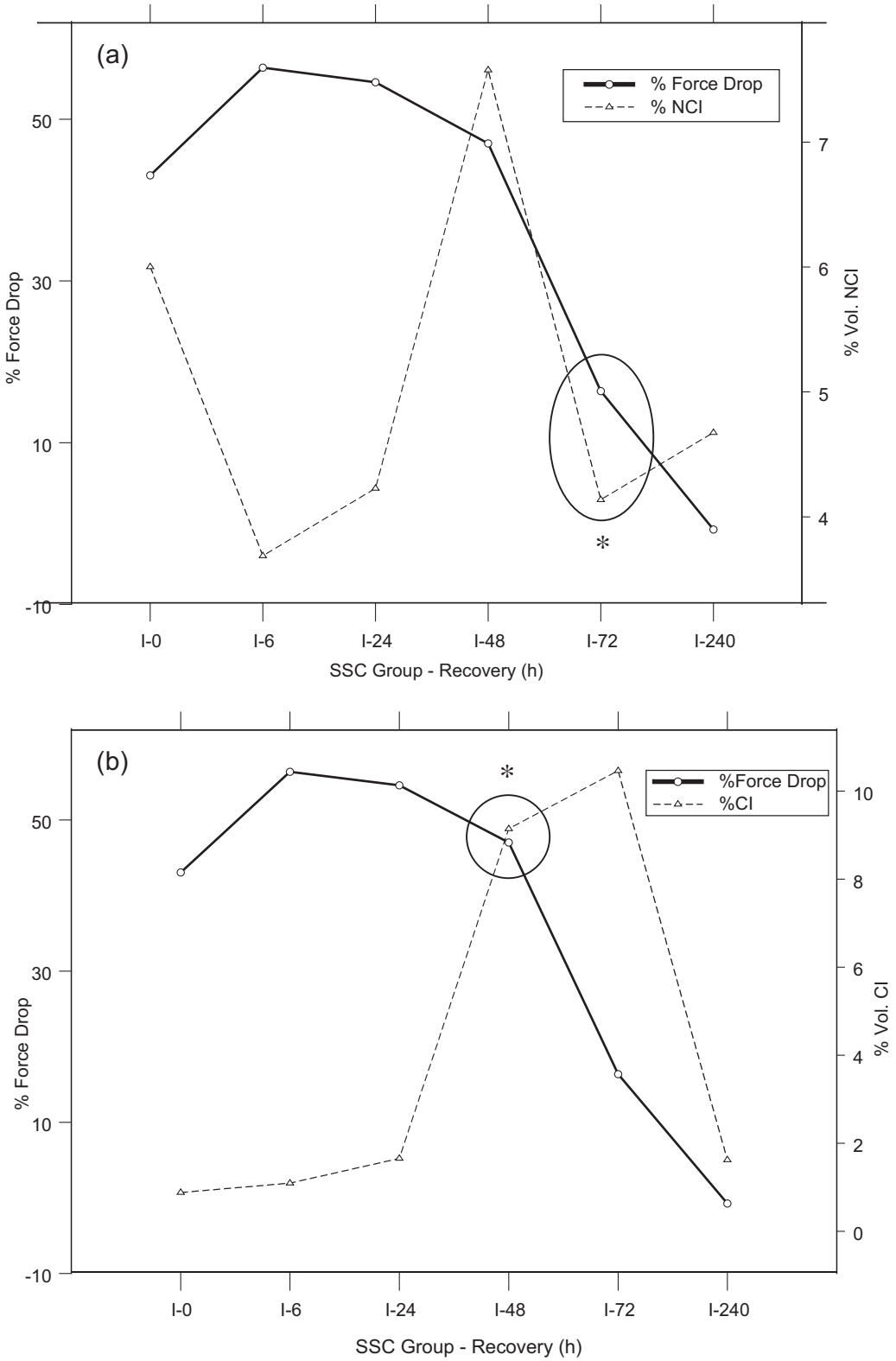

Fig. 8. (*concluded*).

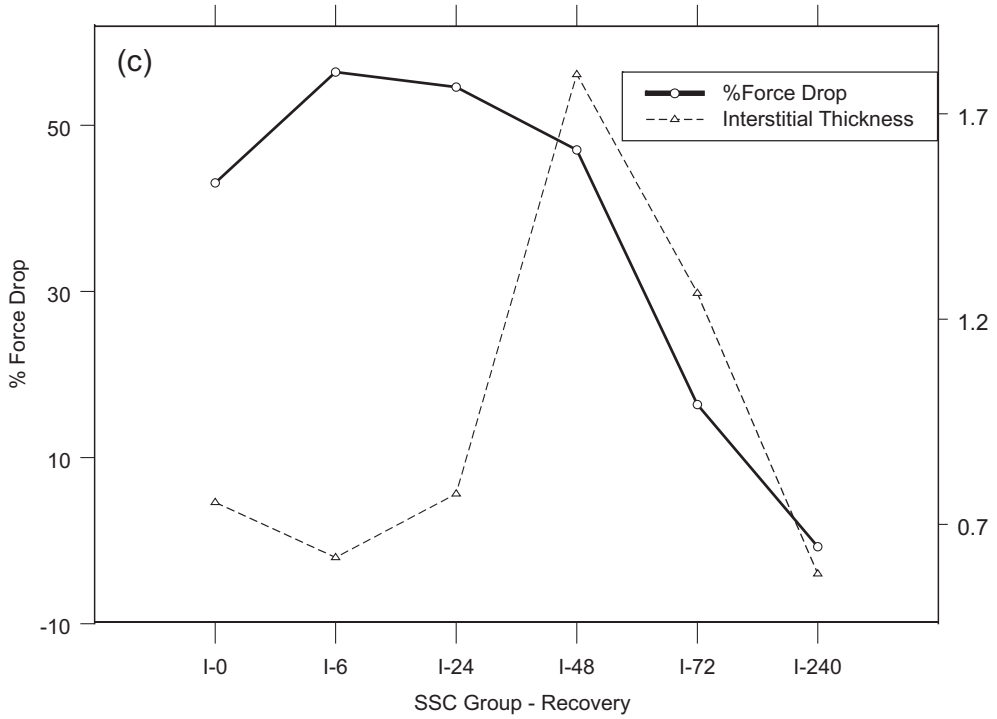

interstitial space were highly consistent with that seen in general histological examination (Geronilla et al. 2003) but yielded quantitative results.

Although previous stereological methods have examined cellular structure and organization of skeletal muscle (Baranska 1997), they have not attempted to directly quantify the degree of myofiber degeneration and inflammation in the tissue concurrently. Moreover, a concern arises at the ultrastructural level regarding the procedure used to identify the functional deficit. One study in particular conducted by Lieber and colleagues (Lieber et al. 1994), reported a significant negative correlation between maximum tetanic tension and the percentage of desmin-negative fibers in the TA and EDL of rabbits. The histological and contractile performance results 1 and 2 d following exposure to eccentric exercise were presented for a subset of muscles. They reported that infiltration of inflammatory cells was present, but did not attempt to characterize the influence that cellular infiltration had on tetanic tension.

In addition, there are a paucity of studies quantifying both myofiber degeneration and inflammation following contraction-induced muscle injury (Friden et al. 1983); (McCully and Faulkner 1985). Our ability to quantify myofiber degeneration and inflammatory processes directly and their relationship to the quantified functional decrements can yield temporal insight into the role myofiber degeneration and inflammation plays in repair and recovery. While some histological approaches and techniques have been termed "too insensitive" to demonstrate the ability to quantify or detect cellular infiltration as a result of the imposed injury (Faulkner et al. 1989), this stereological technique does so convincingly.

The presence of degenerative (necrotic) myofibers was significant in the TA muscle 24–72 h post-injury. In addition, the percent force drop showed a peak response 6 h post-injury and remained significantly elevated until 72 h. The percent force drop was associated with the percent degenerative myofiber volume and the degenerative myofiber average thickness 48 h post-exposure for the SSC group. If the increased degenerative volume leads to an increased degenerative myofiber thickness, then degenerative thickness may serve a critical purpose in producing modifications in and to the interstitial space. Furthermore, by 240 h post-exposure there was neither an isometric force deficit nor presence of degenerative myofibers in the SSC group, signifying that myofibers were fully recovered from SSC-induced injury at this time. Even though less than 1% of the degenerative myofiber volume existed at 240 h, a non-return to baseline in the degenerative myofiber thickness was evident at 240 h; hence the residual degenerative thickness may be an important determinant of adaptation to the interstitial space.

The importance of inflammation and its contribution in repair and regeneration of skeletal muscle have been considered previously (Tidball et al. 1995), although it's importance is not thoroughly understood. In this study, the NCI response was not evident at early time points, but %volume NCI was significant 48 h post-injury. Interestingly, the increase in %volume NCI was associated with a significant increase in the percent force drop at 72 h. Furthermore, the increase observed in %volume CI at 48 h was also associated with the increase in percent force drop, yet as the isometric force started to recover (percent force drop decreased), the percent CI continued to significantly increase until 72 h post-injury. One explanation is the increase in %volume CI at 48 and 72 h may be indicative of an increase in cellular infiltrates, specifically macrophage (Koh et al. 2003; Lapointe et al. 2002) but not neutrophil infiltration (Pizza 2002), as indicated by the temporal increases observed

in the CI. Even though no association was observed at 48 h for the %volume NCI and percent force drop, or at 72 h for the %volume CI and percent force drop, the interstitial space's average thickness increase was associated with the percent force drop both 48 and 72 h post-injury. Furthermore, it should be noted that an increase in thickness of a degenerating myofiber (myofiber swelling and cellular infiltrates) would be expected, owing to the increased permeability of the myofiber to edema and cellular infiltrates; our results depict this event, as there was an observed increase in the %volume NCI at 48 h and the %volume CI at 48 and 72 h. While the case may indeed be that degenerative myofiber thickness' influence on the interstitial space does not limit the resolution capacity of skeletal muscle, it is plausible that non-cellular and cellular interstium directly influences the interstitial space long-term, and this contributes extensively to the modifications to influence surviving myofibers. Thus, we propose that the non-cellular and cellular interstium is influential in regulating the interstitial space's architecture; and that CI influences on the interstitial space may be a highly sensitive measure for quantifying skeletal muscle's degenerative response. Further investigation is needed to determine the physiological contribution of CI (e.g., specific cell populations influential in regulating the interstitial space and myofiber's response — cell–cell interactions) and interstitial thickness has on SSC-induced injury in additional experimental groups (e.g., aged populations, dietary supplemented populations).

A limitation of the current study, which may be acknowledged for all investigative purposes, is that the results may be relative when comparisons and conclusions are made between species. Thus, we have demonstrated that this standardized stereological technique can rapidly assess, and more importantly quantify, myofiber degeneration, inflammation, and the associated changes occurring in and to the interstitial space temporally in muscle tissue morphologically after exposure to injurious SSCs. Further, these quantitative measurements of myofiber degeneration and inflammation are associated with isometric force deficits observed 24 through 72 h post-injury.

Acknowledgements

The authors thank Dr. Ann Hubbs and Dr. Petia Simeonova of the National Institute for Occupational Safety and Health (NIOSH) and Dr. Stephen Alway of West Virginia University School of Medicine for their critical review and comments regarding this manuscript.

References

Baranska. 1997. Quantitative ultrastructural evaluation of satellite cells in soleus muscles from rats kept in hypokinesia.. Exp. Mol. Pathol. **64**: 13–21.

Bigard, A.X., Merino, D., Lienhard, F., Serrurier, B., and Guezennec, C.Y. 1997. Quantitative assessment of degenerative changes in soleus muscle after hindlimb suspension and recovery. Eur. J. Appl. Physiol. Occup. Physiol. **75**: 380–387.

Cutlip, R.G., Stauber, W.T., Willison, R.H., McIntosh, T.A., and Means, K.H. 1997. Dynamometer for rat plantar flexor muscles in vivo. Med. Biol. Eng. Comput. **35**: 540–543.

Cutlip, R.G., Geronilla, K.B., Baker, B.A., Kashon, M.L., Miller, G.R., and Schopper, A.W. 2004. Impact of muscle length during stretch–shortening contractions on real-time and temporal muscle performance measures in rats in vivo. J. Appl. Physiol. **96**: 507–516.

Devor, S.T., and Faulkner, J.A. 1999. Regeneration of new fibers in muscles of old rats reduces contraction-induced injury. J. Appl. Physiol. **87**: 750–756.

Faulkner, J.A., Jones, D.A., and Round, J.M. 1989. Injury to skeletal muscles of mice by forced lengthening during contractions. Q. J. Exp. Physiol. **74**: 661–670.

Faulkner, J.A., Brooks, S.V., and Zerba, E. 1995. Muscle atrophy and weakness with aging: contraction-induced injury as an underlying mechanism. J. Gerontol. A. Biol. Sci. Med. Sci. **50**(Spec. No.): 124–129.

Friden, J., and Lieber, R.L. 1998. Segmental muscle fiber lesions after repetitive eccentric contractions. Cell Tissue Res. **293**: 165–171.

Friden, J., Sjostrom, M., and Ekblom, B. 1983. Myfibrillar damage following intense eccentric exercise in man. Int. J. Sports Med. **4**: 170–176.

Geronilla, K.B., Miller, G.R., Mowrey, K.F., Wu, J.Z., Kashon, M.L., Brumbaugh, K., et al. 2003. Dynamic force responses of skeletal muscle during stretch–shortening cycles. Eur. J. Appl. Physiol. **90**: 144–153.

Glaser. 2000. Stereology, morphometry, and mapping: the whole is greater than the sum of its parts. J. Chem. Neuroanat. **20**: 115–126.

Hesselink, M.K., Kuipers, H., Geurten, P., and Van Straaten, H. 1996. Structural muscle damage and muscle strength after incremental number of isometric and forced lengthening contractions. J. Muscle Res. Cell Motil. **17**: 335–341.

Koh, T.J., Peterson, J.M., Pizza, F.X., and Brooks, S.V. 2003. Passive stretches protect skeletal muscle of adult and old mice from lengthening contraction-induced injury. J. Gerontol. A. Biol. Sci. Med. Sci. **58**: 592–597.

Komulainen, J., Takala, T.E., Kuipers, H., and Hesselink, M.K. 1998. The disruption of myofibre structures in rat skeletal muscle after forced lengthening contractions. Pflugers Arch, **436**: 735–741.

Komulainen, J., Kalliokoski, R., Koskinen, S.O., Drost, M.R., Kuipers, H., and Hesselink, M.K. 2000. Controlled lengthening or shortening contraction-induced damage is followed by fiber hypertrophy in rat skeletal muscle. Int. J. Sports Med. **21**: 107–112.

Krajnak, K.M.R., Baker, B.A., Geronilla, K.B., Miller, G.R., and Cutlip, R.G. 2004. A novel stereological method used to quantify muscle damage induced by injurious stretch–shortening cycles. Med. Sci. Sports Exerc. **36**(5):1831.

Lapointe, B.M., Frenette, J., and Cote, C.H. 2002. Lengthening contraction-induced inflammation is linked to secondary damage but devoid of neutrophil invasion. J. Appl. Physiol. **92**: 1995–2004.

Lieber, R.L., and Friden, J. 1993. Muscle damage is not a function of muscle force by active muscle strain. J. Appl. Physiol. **74**: 520–526.

Lieber, R.L., Woodburn, T.M., and Friden, J. 1991. Muscle damage induced by eccentric contractions of 25% strain. J. Appl. Physiol. **70**: 2498–2507.

Lieber, R.L., Schmitz, M.C., Mishra, D.K., and Friden, J. 1994. Contractile and cellular remodeling in rabbit skeletal muscle after cyclic eccentric contractions. J. Appl. Physiol. **77**: 1926–1934.

Lieber, R.L., Thornell, L.E., and Friden, J. 1996. Muscle cytoskeletal disruption occurs with in the first 15 min of cyclic eccentric contraction. J. Appl. Physiol. **80**: 278–284.

McCully, K.K., and Faulkner, J.A. 1985. Injury to skeletal muscle fibers of mice following lengthening contractions. J. Appl. Physiol. **59**: 119–126.

McCully, K.K., and Faulkner, J.A. 1986. Characteristics of lengthening contractions associated with injury to skeletal muscle fibers. J. Appl. Physiol. **61**: 293–299.

Pizza, F.X. 2002. Muscle inflammatory cells after passive stretches, isometric contractions, and lengthening contractions. J. Appl. Physiol. **92**: 1873–1878.

Stupka, N., Tarnopolsky, M.A., Yardley, N.J., and Phillips, S.M. 2001. Celluar adaptation to repeated eccentric exercise-induced muscle damage. J. Appl. Physiol. **91**: 1669–1678.

Tidball, J.G., Albrecht, D.E., Lokensgard, B.E., and Spencer, M.J. 1995. Apoptosis precedes necrosis of dystrophin-deficient muscle. J. Cell Sci. **108**(6): 2197–2204.

Underwood, E.E. 1970. Quantatative stereology. Addison–Wesley Publishing Co., Reading, Mass.

Van Der Meulen, J.H., McArdle, A., Jackson, M.J., and Faulkner, J.A. 1997. Contraction-induced injury to the extensor digitorum longus muscles of rats: the role of vitamin E. J. Appl. Physiol. **83**: 817–823.

Vijayan, K., Thompson, J.L., Norenberg, K.M., Fitts, R.H., and Riley, D.A. 2001. Fiber-type susceptibility to eccentric contraction-induced damage of hindlimb-unloaded rat AL muscles. J. Appl. Physiol. **90**: 770–776.

Warren, G.L., Hayes, D.A., Lowe, D.A., and Armstrong, R.B. 1993*a*. Mechanical factors in the initiation of eccentric contraction-induced injury in rat soleus muscle. J. Physiol. **464**: 457–475.

Warren, G.L., Lowe, D.A., Hayes, D.A., Karwoski, C.J., Prior, B.M., and Armstrong, R.B. 1993*b*. Excitation failure in eccentric contraction-induced injury of mouse soleus muscle. J. Physiol. **468**: 487–499.

Warren, G.L., Lowe, D.A., and Armstrong, R.B. 1999. Measurement tools used in the study of eccentric contraction-induced injury. Sports Med. **27**: 43–59.